

SIRT1 promotes macrophage polarization to enhance efferocytosis by regulating TXNIP/NLRP3 inflammasome pathway

Qiao Jiang

Xuzhou Medical College

Tongda Xu

Affiliated Hospital of Xuzhou Medical College

Yang Liu

Xuzhou Medical College

Hong Zhu

Affiliated Hospital of Xuzhou Medical College

Yanfeng Ma

Affiliated Hospital of Xuzhou Medical College

Buchun Zhang

Affiliated Hospital of Xuzhou Medical College

Dongye Li (✉ dongyeli@xzhmu.edu.cn)

Xuzhou Medical College

Research Article

Keywords: SIRT1, macrophage polarization, TXNIP/NLRP3, efferocytosis

Posted Date: February 23rd, 2021

DOI: <https://doi.org/10.21203/rs.3.rs-198697/v1>

License: © ⓘ This work is licensed under a Creative Commons Attribution 4.0 International License.

[Read Full License](#)

Abstract

Objects: This study aimed to determine if SIRT1 could enhance efferocytosis and inhibit apoptosis by modulating cell polarization through the TXNIP/NLRP3 inflammasome pathway in murine peritoneal macrophages.

Methods and Results: The effects of SIRT1 in peritoneal macrophages were detected using adenovirus-mediated overexpression and knockdown of SIRT1. The apoptotic rate was determined by Annexin V/propidium iodide staining. LDL cholesterol levels were tested by Oil Red O staining and cholesterol testing. Efferocytosis of peritoneal macrophages was determined by fluorescence staining and macrophage markers were determined by flow cytometry, western blot, and ELISA. SIRT1 decreased cholesterol intake and the apoptotic rate stimulated with ox-LDL in macrophages, which was consistent with upregulation of Bcl-2 and caspase-3 and downregulation of Bax and cleaved caspase-3. SIRT1 increased efferocytosis in macrophages. Expression levels of the M1 macrophage markers IL-6, TNF- α , iNOS, and CD16/32 were decreased, and levels of the M2 markers Dectin-1, IL-10, Arg-1, and CD206 were increased by SIRT1. Moreover, SIRT1 inhibited the ox-LDL stimulated increase in expression of TXNIP and NLRP3 proteins. The effects of SIRT1 were similar to those of TXNIP/NLRP3 inflammasome pathway inhibitor MCC950.

Conclusions: These results indicated that SIRT1 exerted an anti-atherosclerosis effect by regulating macrophage polarization to enhance efferocytosis and inhibit apoptosis. Specifically, these effects were generated by downregulation of the TXNIP/NLRP3 inflammasome pathway.

Introduction

Atherosclerotic plaque formation is the main pathological basis for acute cardiovascular and cerebrovascular diseases. Preventing the formation and progression of atherosclerotic plaques is thus important for reducing morbidity and mortality due to acute coronary events.

Previous studies have confirmed that apoptosis of smooth muscle cells and macrophages play vital functions in the formation and development of atherosclerotic plaques^{1,2}. Excessive apoptosis is an obvious feature of unstable plaques. Plaque rupture with thrombosis is responsible for the acute clinical symptoms of atherosclerosis, and increased apoptosis can directly cause plaque instability. Timely phagocytosis of apoptotic cells thus aids plaque stabilization, indicating that the ability to clear apoptotic cells may be an important contributor to the clinical events occurring in acute atherosclerotic thrombosis.

Numerous studies have confirmed that the ability of macrophages to clear apoptotic cells, known as efferocytosis, is an important factor related to atherosclerotic plaque progression and acute coronary events³. Macrophages play three main roles in the pathogenesis of atherosclerosis. Macrophages recognize oxidized low-density lipoprotein (ox-LDL) during the initial process of accumulation and modification of arterial endothelial lipid granules. Via monocyte adhesion and migration processes, macrophages are then attracted to the lesion site to phagocytose ox-LDL. Finally, macrophages recognize

and engulf large amounts of lipids via scavenger receptors to form foam cells. When apoptosis occurs, the apoptotic cells can be effectively recognized and phagocytosed by macrophages to prevent lipid accumulation, thereby limiting plaque development. However, many factors, including an inflammatory environment, increased lipid load, and smoking, can reduce macrophage efferocytosis, thus preventing the removal of apoptotic foam cells from the plaque⁴. This suggests that enhancing macrophage efferocytosis by drugs or other methods may help to inhibit vascular plaque progression and reduce acute coronary events.

Atherosclerosis is currently recognized as an inflammatory and immune disease. Macrophages, as innate immune and inflammatory cells with highly heterogeneous and plasticity, participate in the whole process of atherosclerosis. According to the activation mode and immune function of macrophages, they can be divided into two categories: classically activated macrophages (M1 type) and alternative activated macrophages (M2 type). M1 macrophages are involved in antigen presentation, inflammation, and pathogen clearance, while M2 macrophages play a role in inhibiting inflammation and promoting tissue damage repair^{5, 6, 7}. The transformation between inflammatory M1 and anti-inflammatory M2 macrophages thus represents a potential novel target for preventing and treating atherosclerotic disease^{8, 9}.

The nucleotide-binding domain, leucine-rich-repeat-containing family, pyrin domain-containing 3 (NLRP3) inflammatory complex is closely connected with immune inflammation. It can recognize a variety of pathogens and damage signals, and plays significant roles in the occurrence and development of many inflammatory diseases. Thioredoxin (TRX)-interacting protein (TXNIP), a type of TRX-binding protein, is involved in regulating the cell redox state, fighting oxidative stress, activating transcription factors to accelerate cell growth, and inhibiting apoptosis. Expression of the NLRP3 inflammatory complex can be increased by reactive oxygen species (ROS)-mediated TXNIP activation. Furthermore, studies have shown that the NLRP3 inflammatory complex may be involved in the development of the atherosclerotic inflammatory response¹⁰.

Silent mating type information regulation 2 homolog-1 (SIRT1) is a critical nuclear protein with roles in the regulation of mammalian development, cell differentiation, aging, and energy metabolism. SIRT1 is currently thought to slow plaque progression by acting on macrophages, and the natural SIRT1 agonist, resveratrol, has demonstrated anti-atherosclerotic effects^{11, 12, 13}. Resveratrol enhanced macrophage phagocytosis and reduced ox-LDL uptake in RAW264.7 macrophages¹⁴. Moreover, SIRT1/AMPK α signaling was shown to regulate M1/M2 polarization to reduce inflammatory responses in rheumatoid arthritis¹⁵. However, whether SIRT1 can enhance macrophage cytoplasmic regulation of atherosclerotic plaques by inducing the differentiation of M1 into M2 macrophages, and the potential mechanisms involved, remain unclear.

We proposed that SIRT1 may regulate macrophage polarization via the TXNIP/NLRP3 inflammasome pathway to enhance macrophage efferocytosis. This study aimed to investigate the mechanisms

underlying the anti-atherosclerosis effects of SIRT1 on macrophages, and provided an experimental basis for the selection of novel drug targets for atherosclerosis.

Results

Detection of SIRT1 adenovirus infection efficiency

The multiplicity of infection (MOI) of Ad-SIRT1 was determined by fluorescence staining. The positivity rate reached 95% at a MOI of 600, with no further increase with increasing of MOI. Adenovirus infection in this study was therefore carried out at an MOI of 600.

To determine the infection efficiency of Ad-SIRT1, the peritoneal macrophages were divided into four groups: a control group, Ad-NC (adenovirus vector control) group, Ad-SIRT1 group, and Ad-sh-SIRT1 group. SIRT1 protein expression levels were quantified by western blot. Treatment with Ad-SIRT1 significantly increased while Ad-sh-SIRT1 significantly decreased SIRT1 protein expression levels. There was no significant difference between the values in the control and Ad-NC groups (Fig. 1).

Anti-apoptosis effects of SIRT1 in macrophages

We compared the apoptosis rates among the different groups. As shown in Fig. 2A and B, the apoptosis rate was significantly increased following ox-LDL treatment compared with the control group, and this rate was significantly decreased by SIRT1 overexpression. SIRT1 suppression further increased macrophage apoptosis compared with the ox-LDL group. The apoptosis rates in the ox-LDL and ox-LDL + Ad-NC groups were similar. These results indicated that SIRT1 also exerted an anti-apoptosis function.

As shown in Fig. 2C, expression levels of anti-apoptotic (Bcl-2, caspase-3) and pro-apoptotic proteins (Bax, cleaved caspase-3) were detected by western blot. Bax and cleaved caspase-3 levels were increased and Bcl-2 and caspase-3 levels were decreased following ox-LDL treatment compared with the control group. Bax and cleaved caspase-3 protein expression levels were further elevated and Bcl-2 and caspase-3 levels were further reduced in the ox-LDL + Ad-sh-SIRT1 group. In contrast, Bax and cleaved caspase-3 expression levels were reduced and Bcl-2 and caspase-3 protein levels were increased in the ox-LDL + Ad-SIRT1 group. Expression levels of the tested proteins were similar in the ox-LDL and ox-LDL + Ad-NC groups.

Overexpression of SIRT1 inhibited phagocytosis lipid and enhanced macrophage efferocytosis

We stimulated peritoneal macrophages with ox-LDL to induce lipid accumulation and investigated the effects of SIRT1 on lipid phagocytosis by macrophages. Ox-LDL increased lipid accumulation compared with the control group, as shown by Oil Red O staining. Overexpression of SIRT1 significantly decreased intracellular lipid droplets and lipid droplet particles induced by ox-LDL, while the largest number of foam cells, most obvious lipid droplets, and largest volume of lipid droplets were found in the Ad-sh-SIRT1 group. Ox-LDL significantly increased levels of LDL cholesterol compared with untreated cells, as shown by cholesterol testing. Cellular cholesterol intake was significantly decreased by transfection with SIRT1 adenovirus. Treatment with ox-LDL + Ad-sh-SIRT1 further increased the cholesterol intake compared with

the ox-LDL group (Fig. 3A, B and C). These results suggested that SIRT1 inhibited the capacity of macrophages to phagocytose lipid.

We investigated the effects of SIRT1 on peritoneal macrophage efferocytosis by fluorescence staining. As shown in Fig. 3D, the macrophage phagocytic index was decreased in the ox-LDL group compared with the control group, and was further decreased by transfection with Ad-sh-SIRT1. In contrast, Ad-SIRT1 pretreatment significantly increased the ox-LDL-induced reduction in phagocytic index. There was no significant difference in phagocytic index between the ox-LDL and ox-LDL + Ad-NC groups. These results demonstrated an improved effect of SIRT1 on macrophage efferocytosis.

Effects of SIRT1 on macrophage polarization

We investigated the effects of SIRT1 on macrophage polarization by identifying the transformation between inflammatory M1 and anti-inflammatory M2 macrophages.

We evaluated the phenotypic markers of M1 and M2 macrophages (CD16/32 and CD206) by flow cytometry (Fig. 4A and B). The percentage of CD16/32 cells increased after treatment with ox-LDL compared with untreated cells. Furthermore, the percentage of CD16/32 cells was further increased by Ad-sh-SIRT1. Ad-SIRT1 treatment reduced the ox-LDL-induced increase in percentage of CD16/32 cells. In contrast, the percentage of CD206 cells was slightly decreased by ox-LDL. SIRT1 knockdown decreased the percentage of CD206 cells compared with the ox-LDL-treated group, while Ad-SIRT1 treatment increased the percentage of CD206 cells.

We also detected the expression of the phenotypic marker proteins arginase-1 (Arg-1) and inducible nitric oxide synthase (iNOS) (Fig. 4C). iNOS expression was increased and Arg-1 expression was decreased by ox-LDL compared with the control group, and co-treatment with ox-LDL and Ad-sh-SIRT1 further upregulated the expression of iNOS and further decreased the expression of Arg-1. As expected, SIRT1 overexpression suppressed the ox-LDL-induced upregulation of iNOS and downregulation of Arg-1. There was no significant difference in expression levels between the ox-LDL and ox-LDL + Ad-NC groups. Collectively, these results indicated that SIRT1 promoted the transformation from inflammatory M1 to anti-inflammatory M2 macrophages.

Expression levels of macrophage phenotypic markers were analyzed by ELISAs. As shown in Fig. 4D, Ox-LDL treatment induced a significant increase in M1 markers compared with the control group, whereas marker levels were significantly decreased in the Ad-SIRT1 group compared with the ox-LDL group. Marker expression was further increased in the Ad-sh-SIRT1 group compared with the ox-LDL-treated group. There was no significant difference in marker levels between the ox-LDL-treated and ox-LDL + Ad-NC groups. Expression levels of M2 markers were slightly decreased in the ox-LDL-treated group, and these were further downregulated in the Ad-sh-SIRT1 group. In contrast, marker expression was enhanced in the Ad-SIRT1 group compared with the ox-LDL group. Levels in the ox-LDL-treated and ox-LDL + Ad-NC groups were similar.

Effects of SIRT1 on TXNIP/NLRP3 pathway in macrophages

We explored the mechanism underlying SIRT1 regulation of macrophage polarization by determining the effect of SIRT1 overexpression on the TXNIP/NLRP3 inflammatory pathway.

ROS expression was upregulated by ox-LDL, as shown by flow cytometry (Fig. 5A and B). The index was further increased by Ad-sh-SIRT1. In contrast, SIRT1 overexpression decreased the expression of ROS compared with the ox-LDL group. There was no significant difference between the ox-LDL and ox-LDL + Ad-NC groups.

TXNIP and NLRP3 protein expression levels were significantly upregulated by ox-LDL, and were further upregulated in the ox-LDL + Ad-sh-SIRT1 group, while preincubation with Ad-SIRT1 significantly decreased TXNIP and NLRP3 protein levels (Fig. 5C and D).

Expression level of IL-1 β was analyzed by ELISA. As shown in Fig. 5E, Ox-LDL treatment induced a significant increase compared with the control group, whereas IL-1 β level was significantly decreased in the Ad-SIRT1 group compared with the ox-LDL group. The expression was further increased in the Ad-sh-SIRT1 group compared with the ox-LDL-treated group. There was no significant difference between the ox-LDL-treated and ox-LDL + Ad-NC groups.

Expression of NLRP3 was significantly increased by ox-LDL, and was inhibited by pretreatment with MCC950 (Fig. 6A). Expression levels of the phenotypic marker proteins iNOS and Arg-1 were detected by western blot. Ox-LDL upregulated iNOS and downregulated Arg-1 protein expression levels, and these effects were enhanced in the ox-LDL + Ad-sh-SIRT1 group. Pretreatment with MCC950 significantly inhibited the effects of ox-LDL on the expression of iNOS and Arg-1 (Fig. 6B and C).

The rate of apoptosis was also significantly increased in ox-LDL-treated compared with untreated cells ($P < 0.001$), and this effect was partly blocked by co-administration of MCC950, leading to a significant decrease in apoptosis rate compared with the ox-LDL group (Fig. 6D). Ox-LDL treatment significantly decreased the macrophage phagocytic index compared with the control group, as shown by fluorescence staining, and this effect of ox-LDL was significantly blocked by MCC950 pretreatment (Fig. 6E).

The above results suggested that the TXNIP/NLRP3 inflammasome pathway was involved in the progression of atherosclerosis, and that the mechanism underlying the anti-atherosclerotic effects of SIRT1 via regulating macrophage function involved inhibition of the TXNIP/NLRP3 inflammatory pathway.

Discussion

Atherosclerosis is a cardiovascular disease that poses a major threat to human health. It is characterized by the accumulation of lipids on the blood vessel wall and the infiltration of immune cells.

Pathophysiological studies have identified arterial endothelial injury and lipid deposition as initiating factors of atherosclerosis. Foam cell formation is a core feature of atherosclerosis pathology^{16,17}. Foam cells are mainly formed by macrophage phagocytosis of cholesterol and lipid peroxides, and these then

form the main component of plaque lipid cores^{2,3}, which in turn play a key role in the formation and development of atherosclerosis. Excessive accumulation of apoptotic cells and insufficient phagocytic clearance of macrophages have been suggested to be the main causes of the formation and development of unstable plaques in atherosclerosis. Reducing the entry of extracellular cholesterol into cells, reducing foam cell formation, and enhancing macrophage efferocytosis may delay the progression of atherosclerosis^{18,19}. The current study explored the anti-atherosclerosis effects and mechanism of SIRT1 in primary mouse peritoneal macrophages.

SIRT1 inhibits atherosclerosis

Silent information regulator 2 (Sir2) is a newly discovered NAD⁺ dependent deacetylase, and there are currently at least seven mammalian Sir2 homologs (SIRT1–SIRT7). Among these, SIRT1 shows the highest homology with Sir2, and is widely present in various somatic and germ cells. SIRT1 is an important nuclear protein involved in the regulation of metabolism, inflammation, oxidative stress, cellular senescence, and apoptosis. Previous studies showed that the SIRT1 agonist, resveratrol, had anti-atherosclerotic effects¹⁴. SIRT1 can also enhance macrophage phagocytosis, reduce macrophage ox-LDL uptake and reduce intracellular lipid deposition²⁰. However, the mechanism by which SIRT1 enhances macrophage phagocytosis to slow plaque progression is unclear.

In this study, we showed that SIRT1 reduced macrophage lipid phagocytosis and inhibited apoptosis during the formation of foam cells, while enhancing macrophage efferocytosis to achieve phagocytosis of apoptotic cells, thus inhibiting foam macrophage generation and the formation and development of atherosclerotic plaques.

SIRT1 exerts anti-atherosclerosis effects by regulating macrophage polarization.

As innate immune and inflammatory cells, macrophages are involved in the whole process of atherosclerosis. Macrophages can differentiate into M1 or M2 macrophages, according to their activation mode and immune function. M1 macrophages express IL-6 and Dectin1, underexpress IL-10, secrete inflammatory cytokines including TNF- α and IL-1 β , participate in antigen presentation, and express iNOS and ROS, which are involved in the inflammatory response and pathogen clearance. In contrast, M2 macrophages overexpress the inflammatory inhibitory factors IL-10 and TNF- β , scavenger receptor, mannose receptor, galactose receptor, and Arg-1, inhibit the inflammatory response, and promote tissue damage repair^{21,22}. M1 and M2 macrophages both exist in atherosclerotic lesions. M1 and M2 macrophages can be transformed under certain conditions, and it was recently shown that regulating the transformation of M1 into M2 macrophages allowed macrophages to exert their immune defense function and clear apoptotic and necrotic cells, and thus actively maintain the stability of atherosclerotic plaques. Statins, peroxisome proliferator-activated receptors, and other drugs have been shown to induce M1 macrophages to differentiate into M2 macrophages, and to promote this transformation by regulating the functional differentiation of macrophages^{23,24}. This transformation reduces M1-induced inflammatory damage to the vessel wall and increases the anti-inflammatory abilities of M2

macrophages to promote the repair of atherosclerotic inflammation^{25,26}. This previous study also found that the angiotensin II-1 receptor accelerated the progression of renal atherosclerosis by regulating the proportion of M1/M2 macrophages and affecting macrophage efferocytosis²⁷.

The current results showed that expression levels of the M1 macrophage phenotype markers IL-6, TNF- α , and iNOS were significantly increased by ox-LDL, while expression levels of the M2 markers IL-10, Dectin-1, and Arg-1 were decreased, macrophage apoptosis increased, and cytotoxicity decreased. The above results were reversed by SIRT1 overexpression. These results indicated that SIRT1 regulated macrophage phenotypic transformation to antagonize the inflammatory response, thereby reducing apoptosis and enhancing macrophage efferocytosis.

SIRT1 exerts anti-atherosclerosis effect by macrophage polarization via TXNIP/NLRP3 inflammatory pathway.

NLRP3 is one of the most important inflammatory complexes discovered in recent years. Cholesterol crystallization has been shown to participate in the early stage of atherosclerosis by activating the NLRP3 inflammatory complex in macrophages. The NLRP3 inflammatory complex can be produced in large quantities by ROS-mediated TXNIP activation. The TRX system is a widely distributed NADPH-dependent disulfide reductase system consisting of TRX, TRX reductase, and reduced coenzyme II (NADPH II). TRX is the main cellular antioxidant stress molecule protecting tissues or cells from multiple stimuli. TXNIP is a TRX-binding protein that mediates oxidative stress, suppresses cell proliferation, and induces apoptosis by inhibiting the function of the TRX system. Previous studies showed that myocardial ischemia-reperfusion injury leads to a massive release of ROS, while TXNIP mediates the abnormal activation of the NLRP3 inflammatory complex and aggravates the inflammatory response of myocardial ischemia-reperfusion injury²⁸. In addition, resveratrol has been shown to promote SIRT1 expression to inhibit ROS production and reduce ischemic oxidative stress in the heart.

We investigated the role of the TXNIP/NLRP3 pathway in the inhibitory effect of SIRT1 through macrophage polarization using the NLRP3 inhibitor MCC950. We showed that ox-LDL stimulation significantly increased ROS level, IL-1 β level, TXNIP and NLRP3 protein expressions in macrophages, and that these effects were reversed by SIRT1 overexpression. Ox-LDL treatment shifted the macrophage phenotype from M2 to M1, attenuated macrophage efferocytosis, and increased macrophage apoptosis, whereas ox-LDL combined with SIRT1 or MCC950 pretreatment decreased the proportion of M1 macrophages and increased M2 macrophages, thus enhancing the increased macrophage efferocytosis and reducing macrophage apoptosis. SIRT1 thus exerted an anti-atherosclerosis effect by inhibiting the TXNIP/NLRP3 inflammatory pathway.

In summary, SIRT1 regulated macrophage polarization to enhance macrophage efferocytosis, inhibit macrophage lipid uptake, and reduce apoptosis. The underlying mechanisms of SIRT1 may involve inhibition of the TXNIP/NLRP3 inflammatory pathway, which could provide novel ideas and targets for the treatment of atherosclerosis.

Materials And Methods

All methods were carried out in accordance with relevant guidelines and regulations, and a statement confirming the study was carried out in compliance with the ARRIVE guidelines.

Animals and reagents

C57BL/6 mice (8 weeks old) were provided by the Laboratory Animal Center of Xuzhou Medical University (Xuzhou, China), all experimental protocols were approved by the Laboratory Animal Ethics Committee of Xuzhou Medical University.

Ox-LDL and SIRT1 were purchased from Sigma-Aldrich (St. Louis, MO, USA). SIRT1 was dissolved in dehydrated alcohol as a 25 mM stock solution, and then serially diluted in phosphate-buffered saline (PBS) immediately prior to the experiments. Fetal bovine serum (FBS) and Dulbecco's Modified Eagle Medium (DMEM) were purchased from Gibco BRL (Grand Island, NY, USA). Enzyme-linked immunosorbent assay (ELISA) kits for tumor necrosis factor (TNF)- α and interleukin (IL)-6 were obtained from KeyGEN Bioengineering Institute (Nanjing, China), and ELISA kits for IL-10 was purchased from R&D Systems (Minneapolis, MN, USA). The Annexin V-propidium iodide (PI) apoptosis detection kit was also obtained from KeyGEN Bioengineering Institute. Antibodies against CD16/32 and CD206 were purchased from BioLegend (San Diego, CA, USA). The NLRP3 inhibitor MCC950 and other antibodies were purchased from Cell Signaling Technology Inc. (Danvers, MA, USA).

Culture and treatment of peritoneal macrophages

Peritoneal macrophages were obtained from 2 mice by irrigating the abdominal cavity with PBS at 4°C for 10 minutes, gently massaging the abdominal cavity for 5–10 minutes, and then leaving to stand for 3–5 minutes. Macrophages in the peritoneal cavity were seeded in a 24-well plate (5×10^5 cells/well). The peritoneal macrophages were cultured in DMEM supplemented with 10% heat-inactivated FBS and maintained for 4 hours in 5% CO₂ at 37°C. The plates were washed with pre-warmed PBS to remove non-adherent cells. After culture 12 hours, the adhesive cells were exposed to various experimental treatments and divided into five groups: control group, ox-LDL group, ox-LDL + Ad-NC (adenovirus vector control) group, ox-LDL + Ad-SIRT1 group, and ox-LDL + Ad-sh-SIRT1 group.

Virus transfection experiment

The SIRT1 adenovirus was synthesized by Hanbio Biotechnology Co., Ltd (Shanghai, China). MOI (Multiplicity of Infection) refers to the number of viruses infected per cell. According to the adenoviral vector manipulation manual, Number of viruses = number of cells at the time of transfection \times MOI. Virus volume = virus count / virus titer. The infection experiment was divided into four groups: MOI = 200, 400, 600 and 800. The number of peritoneal macrophages in each group was 2×10^5 , and the control viral vectors with the same titer and volume were added respectively: 4ul, 8ul, 12ul, 16ul, and then each group was infected with 500ul culture medium. Each MOI value adds two holes. After 2 hours of infection, the peritoneal macrophages were replaced with fresh culture medium. After 36 hours of infection, the expression of GFP/RFP was observed by fluorescence microscopy. Five microscopic pictures were

selected to calculate the cell transfection rate in different experimental groups, and the optimal MOI was selected for virus infection experiment.

Oil red o staining

Peritoneal macrophages were washed three times with PBS and then fixed with 4% polyformaldehyde for 10 minutes. After washing with double-distilled water, the cells were stained with Oil Red O solution at 37°C for 20–30 minutes, followed by hematoxylin for 10 minutes after sealing. The cells were photographed under a microscope and analyzed using an Image J analysis system.

Flow cytometry

Peritoneal macrophages (density about 1.3×10^5) were inoculated in 6-well plates, cultured for 24 hours, and then pretreated with different drugs. The cells were then centrifuged and resuspended in DMEM supplemented with 10% FBS to reach a density of $1 \times 10^6/\text{mL}$. Cells were then incubated in the presence of 10 μL Annexin V-fluorescein isothiocyanate and 5 μL PI for 15 minutes in the dark at room temperature, and processed for flow cytometry within 1 hour using a FACSsort (BD Biosciences, Franklin Lakes, NJ, USA) to measure fluorescence intensities. Annexin V/PI-apoptotic cells were counted and the apoptotic ratio was quantified using BD FACS software.

The treated cells were collected as above and incubated with 5 μL of fluorescein isothiocyanate-labeled CD16/32 antibody and 5 μL of phycoerythrin-labeled CD206 antibody for 15 minutes in the dark at room temperature. The fluorescence intensities of the stained cells were then detected by flow cytometry.

The treated cells were collected as above and incubated with 5 μL of ROS antibody for 15 minutes in the dark at room temperature. The fluorescence intensities of the stained cells were then detected by flow cytometry.

Elisas

Levels of the relevant cytokines and growth factors (IL-6, TNF- α , Dectin-1, IL-10, IL-1 β) were measured in M1 and M2 macrophage supernatants using ELISA kits according to the manufacturer's instructions.

Western blotting

Expression levels of selected proteins were detected by western blotting. Equal amounts of proteins extracted from treated cells were loaded into the wells of an 8–15% sodium dodecyl sulfate polyacrylamide gel, separated, and transferred to a polyvinylidene fluoride membrane. The membrane was blocked with 5% blocking solution for 2 hours at room temperature and then incubated with primary antibodies against the target proteins at 4°C overnight. After washing with tris buffered saline containing 0.1% Tween 20 for 3 times (10 minutes each), the membranes were incubated with secondary antibody for 2 hours at room temperature and washed again. The protein bands were then visualized using nitro blue tetrazolium and 5-bromo-4-chloro-3-indolyl-phosphate. Finally, the relative band intensities were measured using Image J analysis system with β -actin as an internal standard to allow direct comparisons among the experimental groups.

Fluorescent staining

Peritoneal macrophages treated by different experiments were labeled with carboxyfluorescein diacetate succinimide green cell tracer and apoptotic cells were labeled with PI red tracer. After incubation (5% CO₂ and 95% N₂) for 2 hours at 37°C, the cells were washed with PBS and then fixed with 4% paraformaldehyde. Apoptotic cells were observed by fluorescence microscopy. The combination of green and red markers into yellow was considered to be phagocytosis. Phagocytic index = (number of phagocytized cells/number of total cells) x 100.

Statistical analysis

Statistical analyses were performed using GraphPad Prism 5.0 (GraphPad Software, San Diego, CA, USA). Data were expressed as mean ± standard error. The results were analyzed using one- or two-way analysis of variance (ANOVA), followed by Student-Newman-Keuls post-hoc tests. $P < 0.05$ was considered statistically significant.

Declarations

Data availability

The data used to support the findings of this study are available from the corresponding author upon request.

Conflict of interest

None of the authors had a conflict of interest.

Authors' contributions

Qiao Jiang, Tongda Xu, Buchun Zhang, and Dongye Li designed the experiments and analysed the data. Qiao Jiang, Tongda Xu, Yang Liu, Hongzhu, Yanfeng Ma conducted the experiments and contributed to data analysis. Qiao Jiang and Tongda Xu wrote the manuscript. Dongye Li and Buchun Zhang critically revised the manuscript.

Acknowledgments

This work was supported by National Natural Science Foundation of China (81570326), Natural Science Foundation of Jiangsu Province (BK20141139) and Xuzhou science and technology planning project (KC17094).

References

1. Yuan Y, Li P, Ye J. Lipid homeostasis and the formation of macrophage-derived foam cells in atherosclerosis. *Protein Cell*. **3**, 173-181 (2012).
2. Moore KJ, Tabas I. Macrophages in the pathogenesis of atherosclerosis. **145**, 341-355 (2011).

3. Thorp E, Subramanian M, Tabas I. The role of macrophages and dendritic cells in the clearance of apoptotic cells in advanced *Eur J Immunol*.**41**, 2515-2518 (2011).
4. Tabas I. Macrophage death and defective inflammation resolution in atherosclerosis. *Nat Rev Immunol*.**10**, 36–46 (2010).
5. Andrés V, Pello OM, Silvestre-Roig C. Macrophage proliferation and apoptosis in atherosclerosis. *Curr Opin Lipidol*.**23**, 429-438 (2012).
6. Stöger JL, et al. Distribution of macrophage polarization markers in human atherosclerosis. *Atherosclerosis*.**225**, 461-468 (2012).
7. Bouhrel MA, Derudas B, Rigamonti E, Dièvert R, Brozek J, Haulon S, et al. PPARgamma activation primes human monocytes into alternative M2 macrophages with anti-inflammatory properties. *Cell Metab*.**6**, 137-143(2007).
8. Liberale L, Dallegri F, Montecucco F, Carbone F. Pathophysiological relevance of macrophage subsets in atherogenesis. *Thromb Haemost*. 117, 7-18(2017).
9. Nagenborg J, Goossens P, Biessen EAL, Donners MMPC. Heterogeneity of atherosclerotic plaque macrophage origin, phenotype and functions: Implications for treatment. *Eur J Pharmacol*. 816, 14-24(2017).
10. Grebe A, Hoss F, Latz E. NLRP3 Inflammasome and the IL-1 Pathway in Atherosclerosis. *CircRes*. 122, 1722-1740(2018).
11. Alexander Breitenstein¹, Sokrates Stein¹, Erik W Holy¹, Giovanni G Camici¹, Christine Lohmann¹, Alexander Akhmedov, et al. Sirt1 inhibition promotes in vivo arterial thrombosis and tissue factor expression in stimulated cells. *Cardiovasc Res*.**89**, 464-472(2011).
12. Stein S, Matter CM. Protective roles of SIRT1 in atherosclerosis[J]. *Cell Cycle*. **10**, 640-647(2011).
13. Kotas ME, Gorecki MC, Gillum MP. Sirtuin-1 is a nutrient-dependent modulator of inflammation. **2**, 113-118(2013).
14. Liu B, Zhang B, Guo R, Li S, Xu Y. Enhancement in efferocytosis of oxidized low-density lipoprotein-induced apoptotic RAW264.7 cells through Sirt1-mediated autophagy. *Int J Mol Med*. **33**, 523-533(2014).
15. Park SY, et al. SIRT1/Adenosine Monophosphate-Activated Protein Kinase α Signaling Enhances Macrophage Polarization to an Anti-inflammatory Phenotype in Rheumatoid Arthritis. *Front Immunol*.**8**, 1135(2017).
16. Yao BC, Meng LB, Hao ML, Zhang YM, Gong T, Guo ZG, et al. Chronic stress: a critical risk factor for atherosclerosis. *J Int Med Res*.**47**, 1429-1440(2019).
17. Pryma CS, Ortega C, Dubland JA, Francis GA. Pathways of smooth muscle foam cell formation in atherosclerosis. *Curr Opin Lipidol*.**30**, 117-124(2019).
18. Tajbakhsh A, Rezaee M, Kovanen PT, Sahebkar A. Efferocytosis in atherosclerotic lesions: Malfunctioning regulatory pathways and control mechanisms. *Pharmacol Ther*.**188**, 12-25(2018).

19. Yurdagul A Jr, Doran AC, Cai B, Fredman G, Tabas IA. Mechanisms and Consequences of Defective Efferocytosis in Atherosclerosis. *Front Cardiovasc Med*.**4**, 86(2018).
20. Sokrates S, et al. SIRT1 decreases Lox-1- mediated foam cell formation in atherogenesis. *Eur Heart*. **31**, 2301-2309 (2010).
21. Cheol W. L, et al. Macrophage heterogeneity of culprit coronary plaques in patients with acute myocardial infarction or stable angina. *Am J Clin Pathol*. **139**, 317-322 (2013).
22. Kyu Y. C, et al. The phenotype of infiltrating macrophages influences arteriosclerotic plaque vulnerability in the carotid artery. *Stroke Cerebrovasc Dis*.**22**, 910-918 (2013).
23. Adamson S, Leitinger N. Phenotypic modulation of macrophages in response to plaque lipids. *Curr Opin Lipidol*. **22**, 335–342 (2011).
24. Leitinger N, Schulman IG. Phenotypic Polarization of Macrophages in Atherosclerosis. *Arterioscler Thromb Vasc Biol*.**33**, 1120-1126 (2013).
25. Petteri R, et al. Palmitoylethanolamide Promotes a Proresolving Macrophage Phenotype and Attenuates Atherosclerotic Plaque Formation. *Arterioscler Thromb Vasc Biol*.**38**, 2562-2575 (2018).
26. Bi Y, et al. M2 Macrophages as a Potential Target for Antiatherosclerosis Treatment. *Neural Plast*.6724903 (2019).
27. Suguru Y, et al. Macrophage polarization by angiotensin II-type 1 receptor aggravates renal injury- acceleration of atherosclerosis. *Arterioscler Thromb Vasc Biol*. **31**, 2856-2864 (2011).
28. Yi L, et al. TXNIP mediates NLRP3 inflammasome activation in cardiac microvascular endothelial cells as a novel mechanism in myocardial ischemia/reperfusion injury. *Basic Res Cardiol*.**109**, 415(2014).

Figures

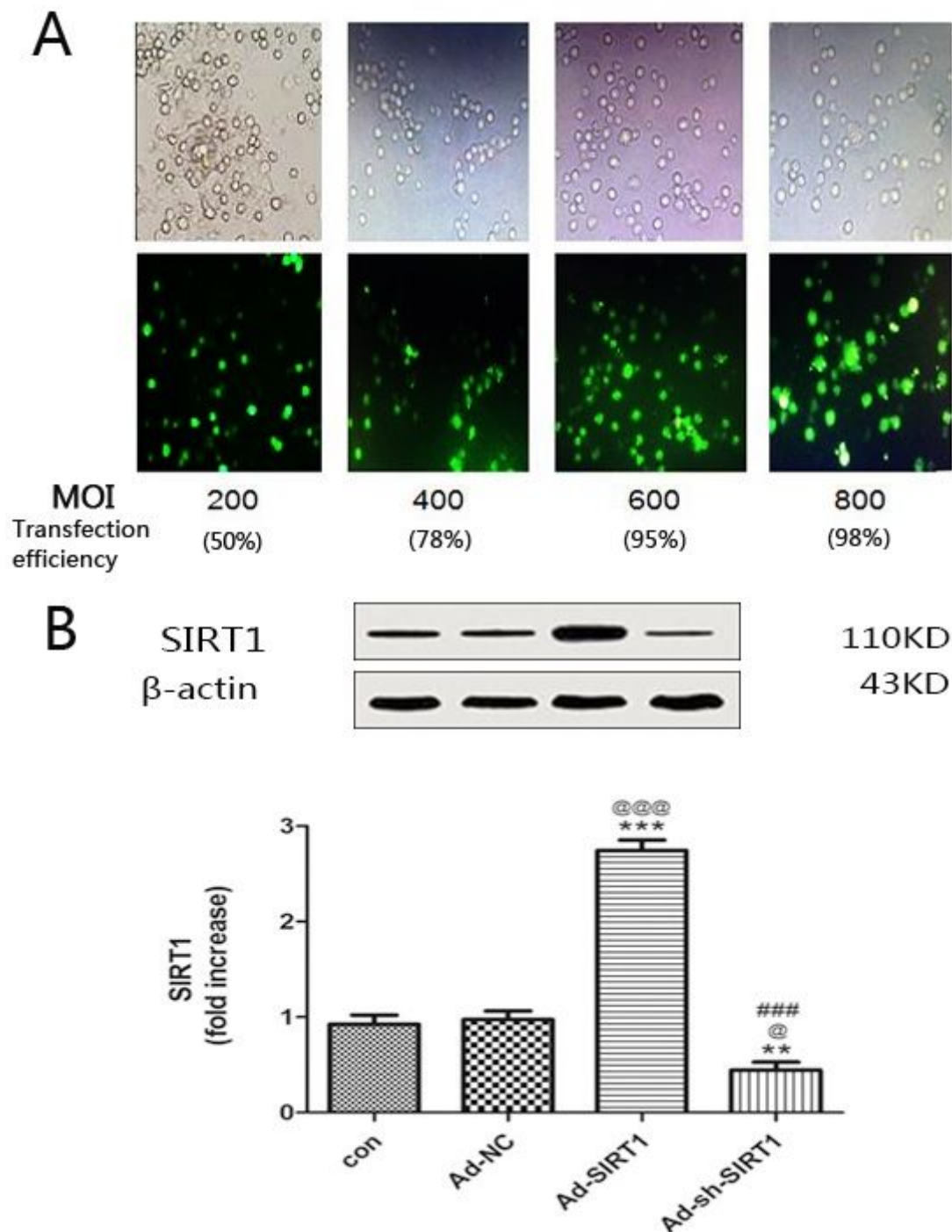


Figure 1

Detection of Silent mating type information regulation 2 homolog-1 (SIRT1) overexpression of adenovirus (Ad-SIRT1) infection efficiency. (A) The adenovirus infection efficiency was detected by fluorescence staining experiments. (B) The adenovirus infection efficiency was detected by Western blot. All data were obtained from three independent experiments. The experiments were performed in three independent runs (n=3). ***p<0.001, **p<0.01, *p<0.05 vs control group. @@@p<0.001, @@p<0.01 vs ox-LDL group. ###p<0.01, #p<0.05 vs ox-LDL+Ad-NC group. &&p<0.01, &p<0.05 vs ox-LDL+Ad-SIRT1 group.

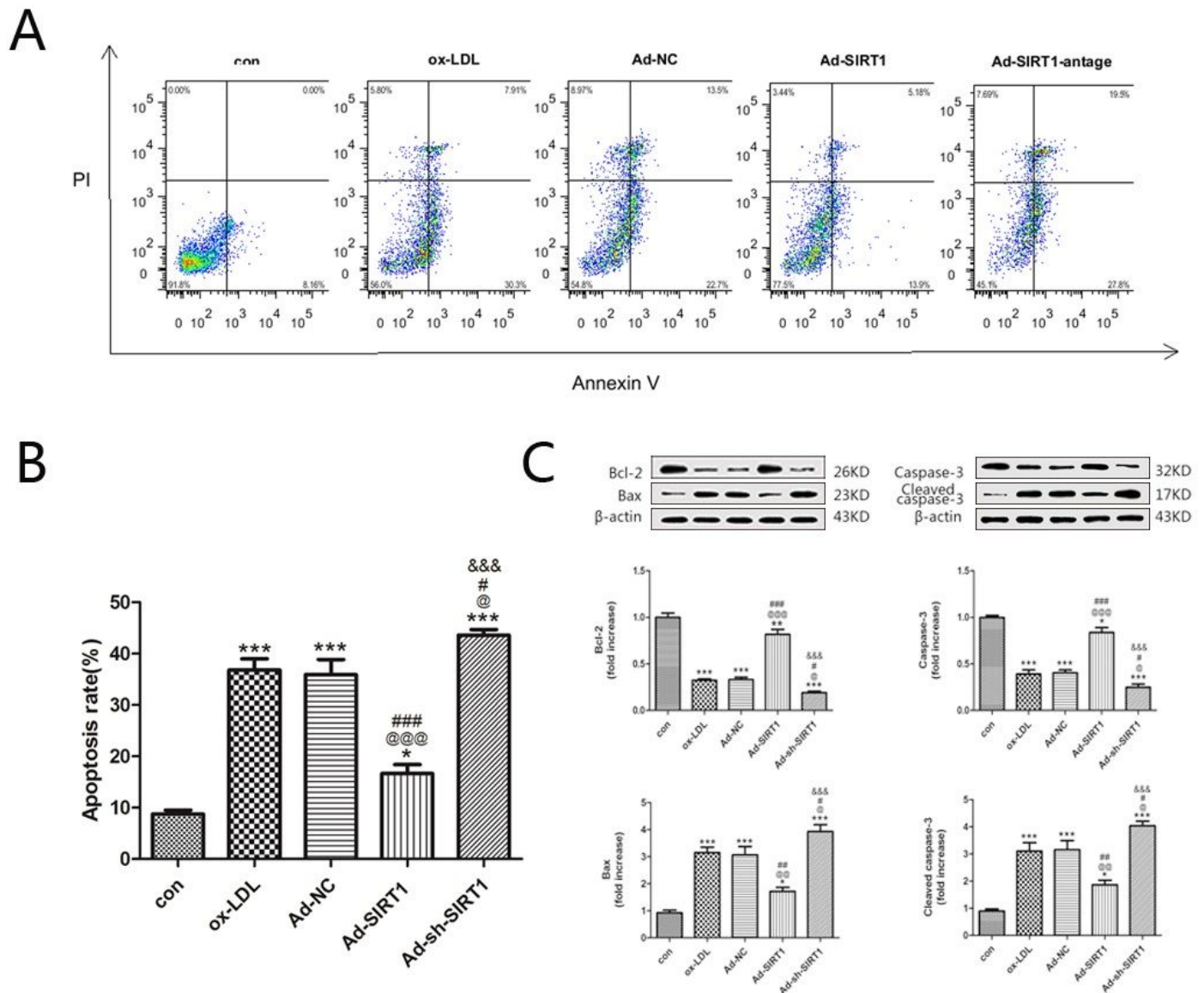


Figure 2

Effects of SIRT1 on oxidized low-density lipoprotein (ox-LDL) induced apoptosis. (A) Flow cytometry was used to observe the apoptosis of macrophages by staining with Annexin V-FITC/PI. (B) The apoptosis ratio was quantified by BD FACS. (C) Representative bands of Bcl-2, Bax, caspase-3, cleaved caspase-3 and quantitative analysis results. The expression of β -actin was measured as an internal control. The experiments were performed in three independent runs ($n=3$). *** $p<0.001$, ** $p<0.01$, * $p<0.05$ vs control group. @@@ $p<0.001$, @@ $p<0.01$ vs ox-LDL group. ## $p<0.01$, # $p<0.05$ vs ox-LDL+Ad-NC group. & $p<0.01$, & $p<0.05$ vs ox-LDL+Ad-SIRT1 group.

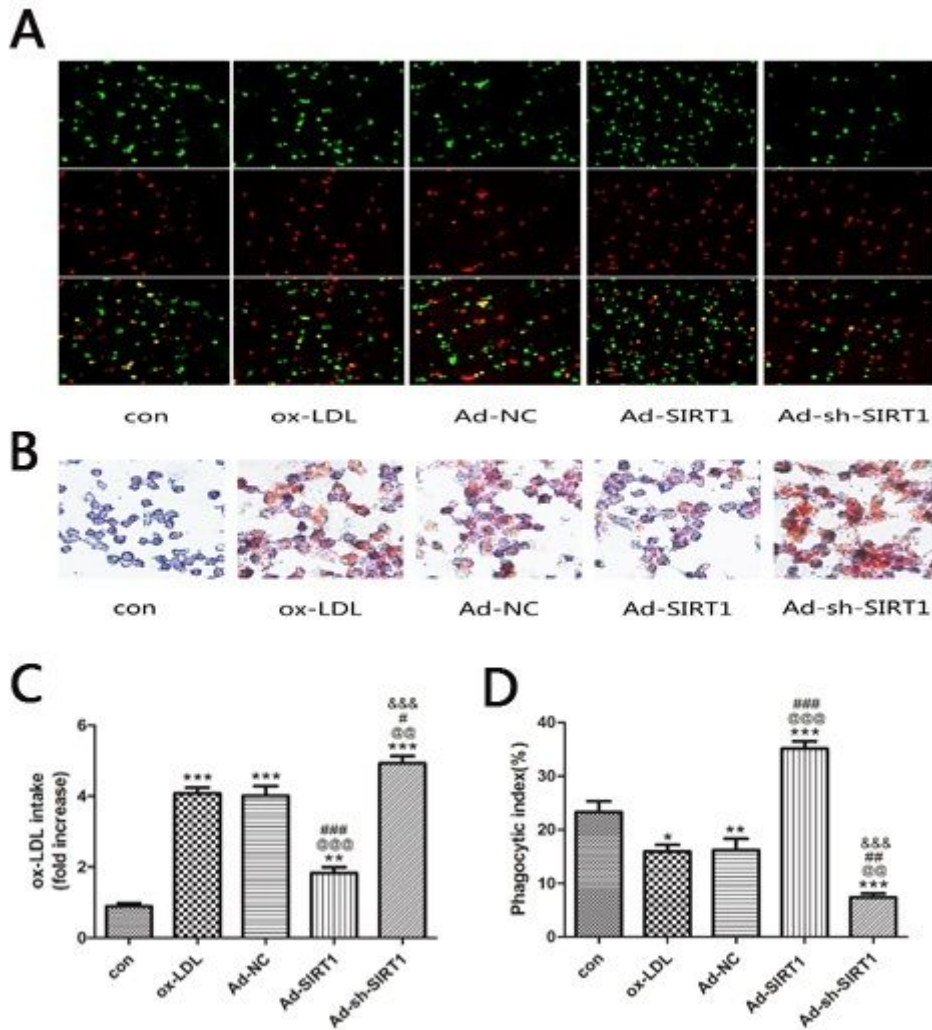


Figure 3

Effects of SIRT1 on macrophage efferocytosis and lipid phagocytosis. (A) Macrophage phagocytic index was detected by fluorescence staining experiments. Red fluorescence represents apoptotic cells using a PI staining. Green CFSE staining fluorescence represents peritoneal macrophages cells. (B) The intake of cholesterol was detected by using Oil Red O staining. (C) The intake of low density lipoprotein cholesterol was measured by cholesterol test kit. Data were expressed as a percentage of the control. The experiments were performed in three independent runs (n=3). ***p<0.001, **p<0.01, *p<0.05 vs control group. @@@p<0.001, @@p<0.01 vs ox-LDL group. ###p<0.01, #p<0.05 vs ox-LDL+Ad-NC group. &p<0.01, &p<0.05 vs ox-LDL+Ad-SIRT1 group. (D) Macrophage phagocytic index was detected by fluorescence staining experiments. The experiments were performed in three independent runs (n=3). ***p<0.001, **p<0.01, *p<0.05 vs control group. @@@p<0.001, @@p<0.01 vs ox-LDL group. ###p<0.001, ##p<0.01 vs ox-LDL+Ad-NC group. &&p<0.001 vs ox-LDL+Ad-SIRT1 group.

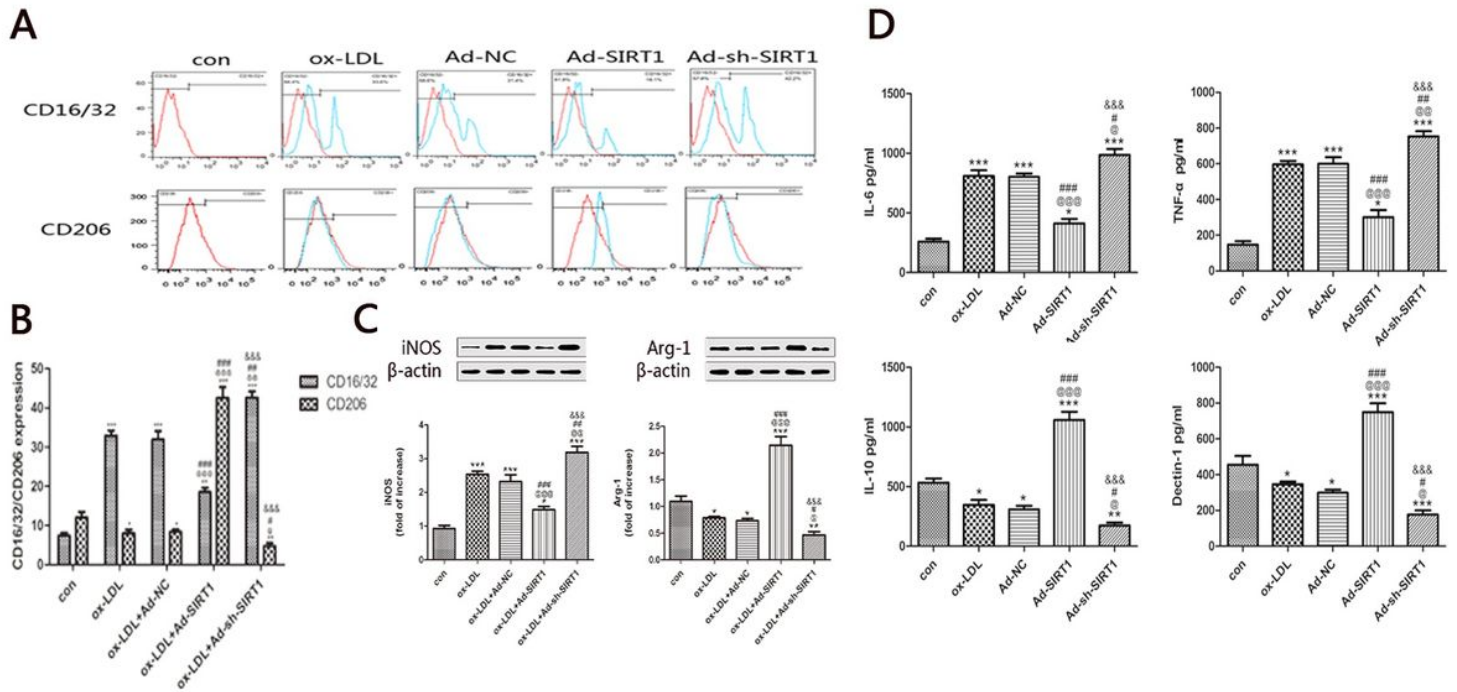


Figure 4

The effects of SIRT1 on macrophage polarization. (A) The expression of M1 (CD16/32) and M2 (CD206) macrophage phenotype markers was detected by flow cytometry. (B) The results were quantified by BD FACS. (C, D) The expression of macrophage phenotype markers. All data were obtained from three independent experiments. The experiments were performed in three independent runs ($n=3$). *** $p<0.001$, ** $p<0.01$, * $p<0.05$ vs control group. @@@ $p<0.001$, @@ $p<0.01$ vs ox-LDL group. ### $p<0.01$, # $p<0.05$ vs ox-LDL+Ad-NC group. && $p<0.01$, & $p<0.05$ vs ox-LDL+Ad-SIRT1 group.

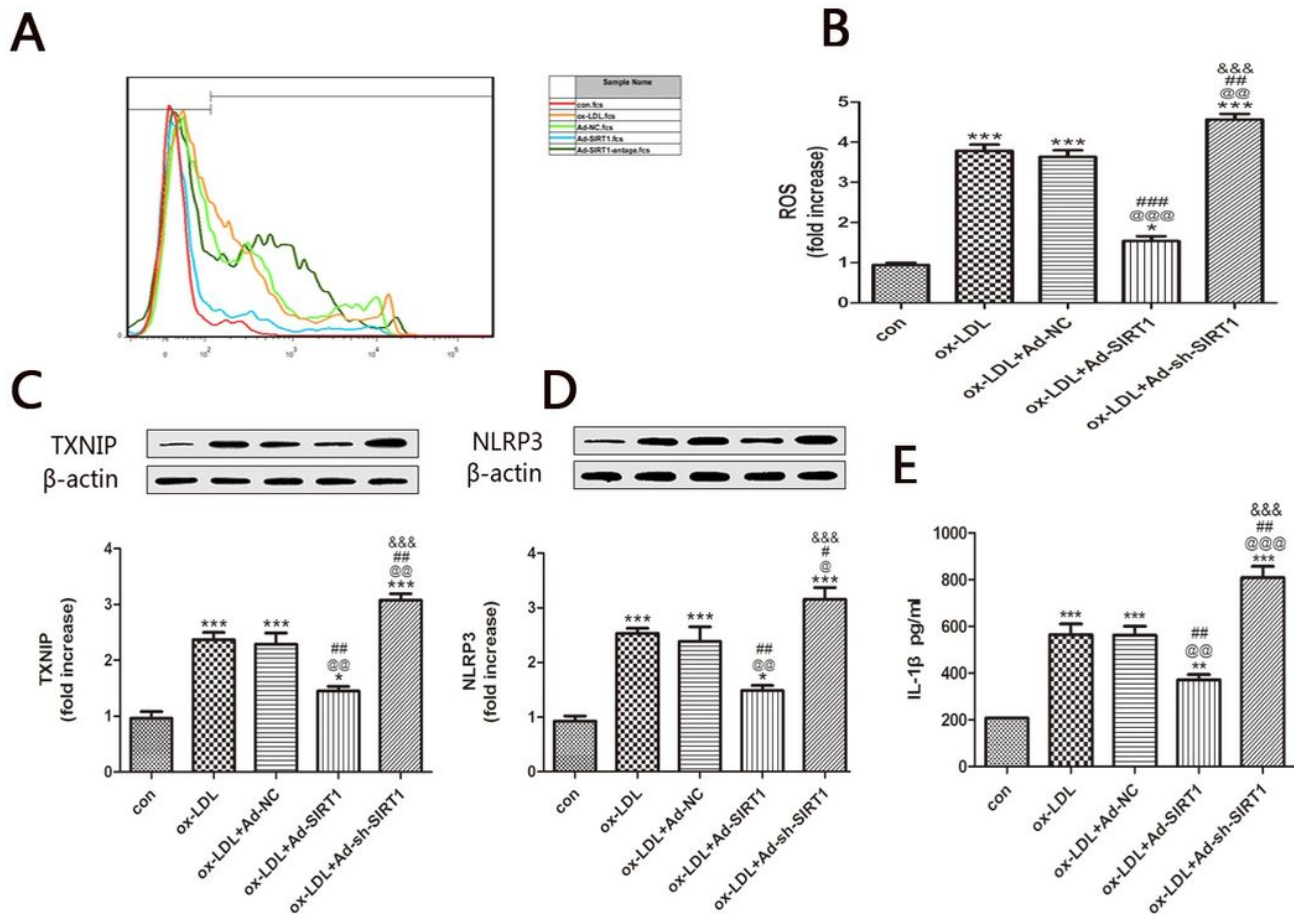


Figure 5

Effects of SIRT1 on TXNIP/NLRP3 pathway in macrophages. (A, B) The expression of ROS was detected by flow cytometry. (C, D) Representative bands of TXNIP and NLRP3 and quantitative analysis results. (E) The expression of IL-1 β was detected by ELISA. The expression of β -actin was measured as an internal control. The experiments were performed in three independent runs (n=3). ***p<0.001, **p<0.01, *p<0.05 vs control group. @@@p<0.001, @@p<0.01 vs ox-LDL group. ##p<0.01, #p<0.05 vs ox-LDL+Ad-NC group. &p<0.01, &p<0.05 vs ox-LDL+Ad-SIRT1 group.

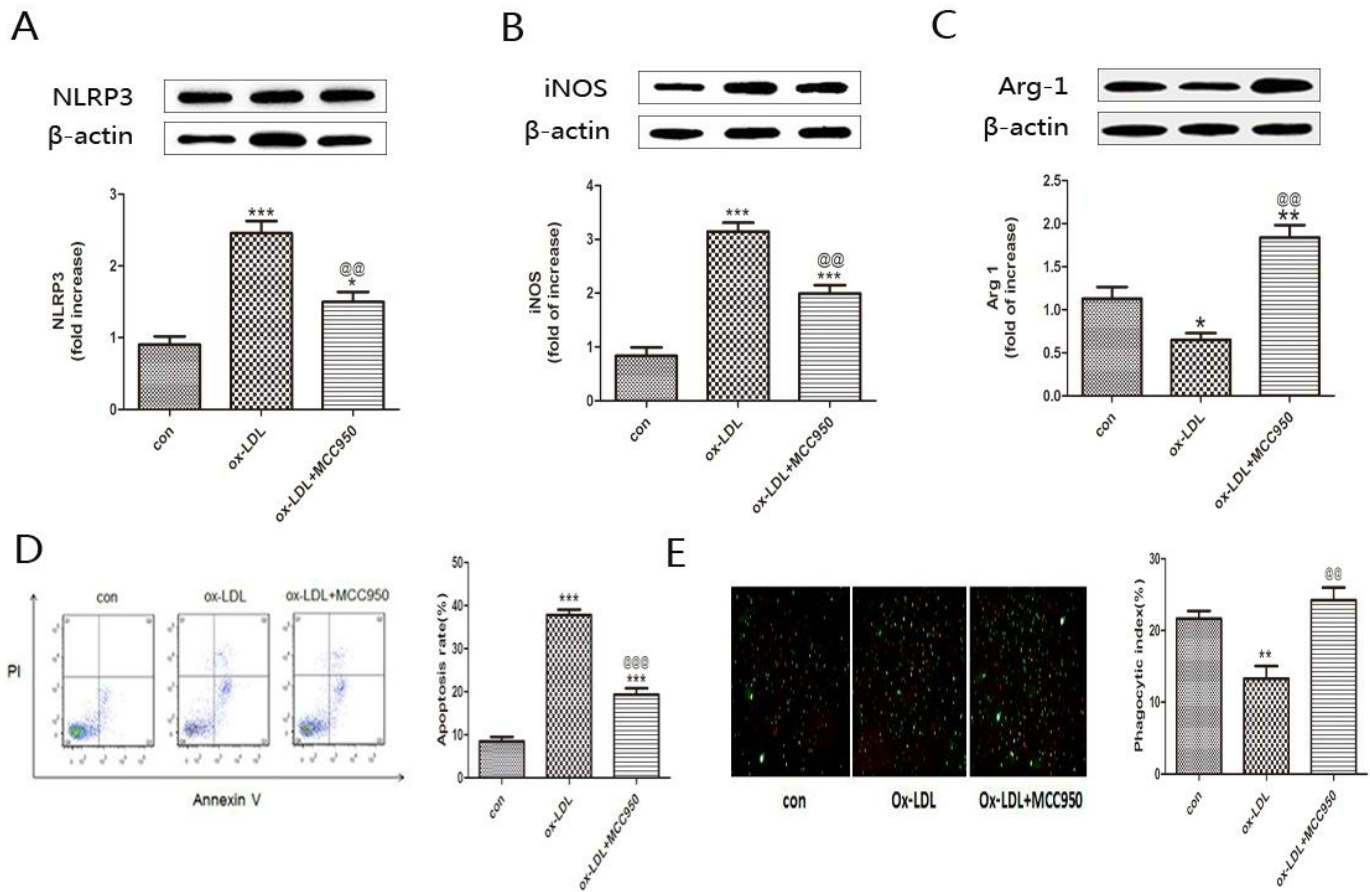


Figure 6

Effects of MCC950 on macrophage efferocytosis and apoptosis. (A, B, C) Representative bands of NLRP3, iNOS and Arg-1 and quantitative analysis results. The expression of β-actin was measured as an internal control. (D) Flow cytometry was used to observe the apoptosis of macrophages by staining with Annexin V-FITC/PI. (E) Macrophage phagocytic index was detected by fluorescence staining experiments. The experiments were performed in three independent runs (n=3). ***p<0.001, **p<0.01 vs control group. @@@p<0.001, @@p<0.01 vs ox-LDL group.